

An Investigation of the Surface Characterization of Laser Surface Remelted and Laser Beam Welded AISI 316L Stainless Steel

Ceyhan KÖSE

Faculty of Natural Sciences and Engineering, Department of Mechanical Engineering, Gaziosmanpaşa University, Tokat, 60150, Turkey

E-mail: ceyhunia@gmail.com, ceyhun.kose@gop.edu.tr

Received: 2 February 2016 / Accepted: 24 February 2016 / Published: 1 April 2016

In this study, AISI 316L austenitic steel was joined by CO₂ laser beam welding method and the microhardness and the surface characteristics of joints were investigated. Also, surface modification was applied on the laser welded and non-welded samples by means of Nd:YAG laser source at laser power 50W, 100W, and 150W. The main materials and the welding seam surfaces of the laser welded samples on which no laser modification had been applied and the surfaces of the samples on which laser surface modification was applied were characterized via SEM, Elemental Mapping, atomic force microscope (AFM), and at the same time, the changes in their surface hardness were identified. As a results, it was identified that the main material surface and the welding seam region of the laser welded sample on which no surface modification had been implemented had less roughness (R_a) than the samples on which laser surface modification had been applied. It was observed that the highest surface roughness belonged to the laser welded sample on which surface modification was applied via 150W laser power. No significant change was observed in the hardness values.

Keywords: Laser beam welding, Laser remelting, Austenitic stainless steel, Surface topography.

1. INTRODUCTION

The Fe-Cr-Ni alloys that contain minimum 10.5% chromium and maximum 1.2% carbon in their chemical compositions are called stainless steel [1]. When nickel is more than 8% in the stainless steel, which is classified into five categories according to its microstructures, makes austenite stable at room temperature, and this type of stainless steel is called austenitic stainless steel [2]. This steel has high mechanical properties and corrosion resistance [3-6].

The simplest austenitic stainless steel whose carbon ratio is reduced in order to improve the corrosion resistance of particles is of class AISI 304L quality. In order to increase the resistance of this

steel against pitting, 2% Mo is added to the alloy, and it is AISI 316L austenitic stainless steel that contains 17-19% chromium and 12-14% nickel; it is used especially in orthopaedic applications and in many branches of the industry [3]. AISI 316L stainless steel is used in many branches of the industry since it has a good combination in terms of its mechanical characteristics, corrosion resistance, and capacity to be welded [3]. The thin and protective chromium oxide layer that forms on the surface of AISI 316L stainless steel leads to corrosion resistance and biocompatibility [7-9]. Since it has high mechanical strength, good corrosion resistance, and is economical, it is commonly used in cardiovascular stents, orthodontic wires [7], and orthopaedic implants [10-12].

Studies that are designed to change the chemistry and physical topography of implant surfaces in order to extend the period of use of the biomedical implants such as AISI 316L stainless steel, and to improve their biocompatibility and osseointegration characteristics [8,13]. One other technique used for surface modification is laser surface remelting. As a result of the quick remelting-solidification that takes place on the surface with by means of the laser surface remelting modification procedure, surface hardness increases, abrasion and corrosion properties improve, a homogeneous surface structure forms, and, at the same time, as a result of an increase in the surface roughness, it results in a positive effect in the implant-tissue interface. In addition to medical field applications, laser surface modification is utilized since it improves the corrosion and abrasion resistance of structural materials [8,13-21]. Laser surface modification is a good choice for improving the resistance against cavitation erosion, pitting corrosion and intergranular corrosion, improvement in internal strains of austenitic stainless steels [22]. After laser surface treatment, the treated surface becomes more resistance to aggressive corrosion environment.

The aim of this study was to investigate the welding seam surface properties of laser welded samples whose surfaces had either been and or not been subjected to Nd:YAG laser modification procedures with the help of SEM, elemental mapping, and AFM in addition to studying the microhardness of the AISI 316L stainless steel that had been joined by CO₂ laser beam welding method.

2. EXPERIMENTAL

2.1. Materials, welding procedure, and laser surface modification procedures

In this study, AISI 316L stainless steel, which is used in many branches of the industry, was used. Table 1 shows the chemical composition of AISI 316L stainless steel.

Table 1. The chemical composition of AISI 316L stainless steel (weight %).

C%	Si	Mn	P	S	Cr	Mo	Ni	Al	Co
0.013	0.528	1.859	0.052	0.0010	16.94	2.065	9.336	0.0020	0.267
Cu	Nb	Ti	V	W	Pb	Sn	Zn	N	Fe
0.248	0.0338	0.014	0.086	0.099	0.0010	0.026	0.027	0.026	68.36

AISI 316L steel plates were butt joined without using any additional metal by means of a TRUMPF LASERCELL 1005 CO₂ laser beam welding machine with 4 kW of power after being attached to the pre-prepared holding stand in line with the parameters given in Table 2. The CO₂ laser beam welding method distinguishes itself from the traditional welding techniques because of its many characteristics such as low heat input, high concentration energy, high welding speed, narrow welding area, deep penetration, compatibility with automation, high mechanical strength, low distortion and the opportunity to weld without using welding wires [23-28].

Table 2. Welding parameters.

Laser power (W)	Travel speed (cm/min)	Shielding gas	Gas flow rate (lt/min)	Focal length (mm)	Heat input (kJ/mm)
4000	180	50% Ar + 50% He	10	200	0.133

The laser surface modification procedures of the samples welded by CO₂ laser beam welding were performed at the parameters specified in Table 3 by means of a micro scale power intensified Pulsed Nd:YAG laser, Rofin Tool Open brand laser welding machine with 150W. Overlapping seams were applied on all of the surfaces CO₂ laser beam welded samples.

Table 3. The laser parameters used in laser surface modification.

Laser power (W)	Travel speed (mm/s)	Pulse duration (ms)	Spot size (mm)	Shielding gas	Gas flow rate (lt/min)	Heat input (kJ/mm)
50	5	5	0.7	Ar	12	0.1
100	5	5	0.7	Ar	12	0.2
150	5	5	0.7	Ar	12	0.3

2.2. Preparation of experimental samples and characterization procedures

After welded and non-welded AISI 316L stainless steel samples joined by CO₂ laser beam were cut in dimensions of 20 x 5 x 3 mm, and then polished with 200-1200 grid sandpaper for characterization studies. The surface properties of the samples were inspected via some hardware that comprised of JEOL JSM 7001 LV brand scanning electron microscope (SEM) and OXFORD X-MAX 80 (EDS+MAPPING). The XRD analysis was performed by utilizing Cu K α radiation rays with a voltage of 40kV and a current of 40mA at a scanning rate of 2°/min with the help of a RIGAKU DMAX-2200/PC brand device. Hardness distribution was measured on a sample (10g oxalic acid +

100 ml pure H₂O) that had been etched electrolytically by adding 200g load to the sinking end of a SHIMADZU brand measuring device. The surface roughness analysis was performed via a BRUKER AFM Q-SCOPE 250/400 brand device at a scanning size of 40μm and a scan rate of 0.5 Hz in tapping mode.

3. RESULTS AND DISCUSSION

3.1. The investigation of the welding area of the laser welded sample and the main material via AFM

Surface texture is an important topic in order to be able to understand the nature of material surfaces and plays an important role in the functional performance of many engineering components [29]. Surface roughness is also a very important parameter for many applications. By characterizing surface roughness, we get information about which application areas that material can be used in effectively. The SEM image of the sample after the main material and welding seam surfaces of the sample, which had been joined by CO₂ laser beam welding method, were polished with sandpaper is shown in Figure 1.

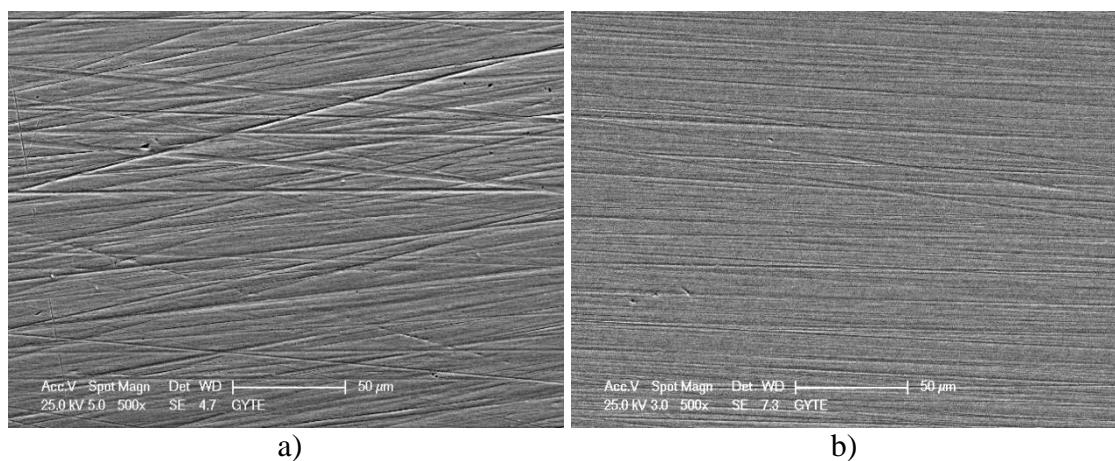


Figure 1. The SEM image of the samples before AFM characterization, a) main material surface, b) welding seam surface of the laser welded sample.

The average surface roughness values (R_a) were identified via AFM analysis performed on the welding seam surface of the welded sample and on any surface of the main material, and the obtained surface topography images were shown in Figure 2. The R_a value obtained on the surface of the main material was 21nm, and the R_a value obtained on the welding seam surface was 22.7nm. Even though the surfaces of the main material and the laser welded sample were prepared under the same condition, the roughness of the welding seam surface of the laser welded sample increased a certain amount. It can be thought that this increase in the roughness occurred because the heat input conducted to the welding area affected the surface texture of the welding seam.

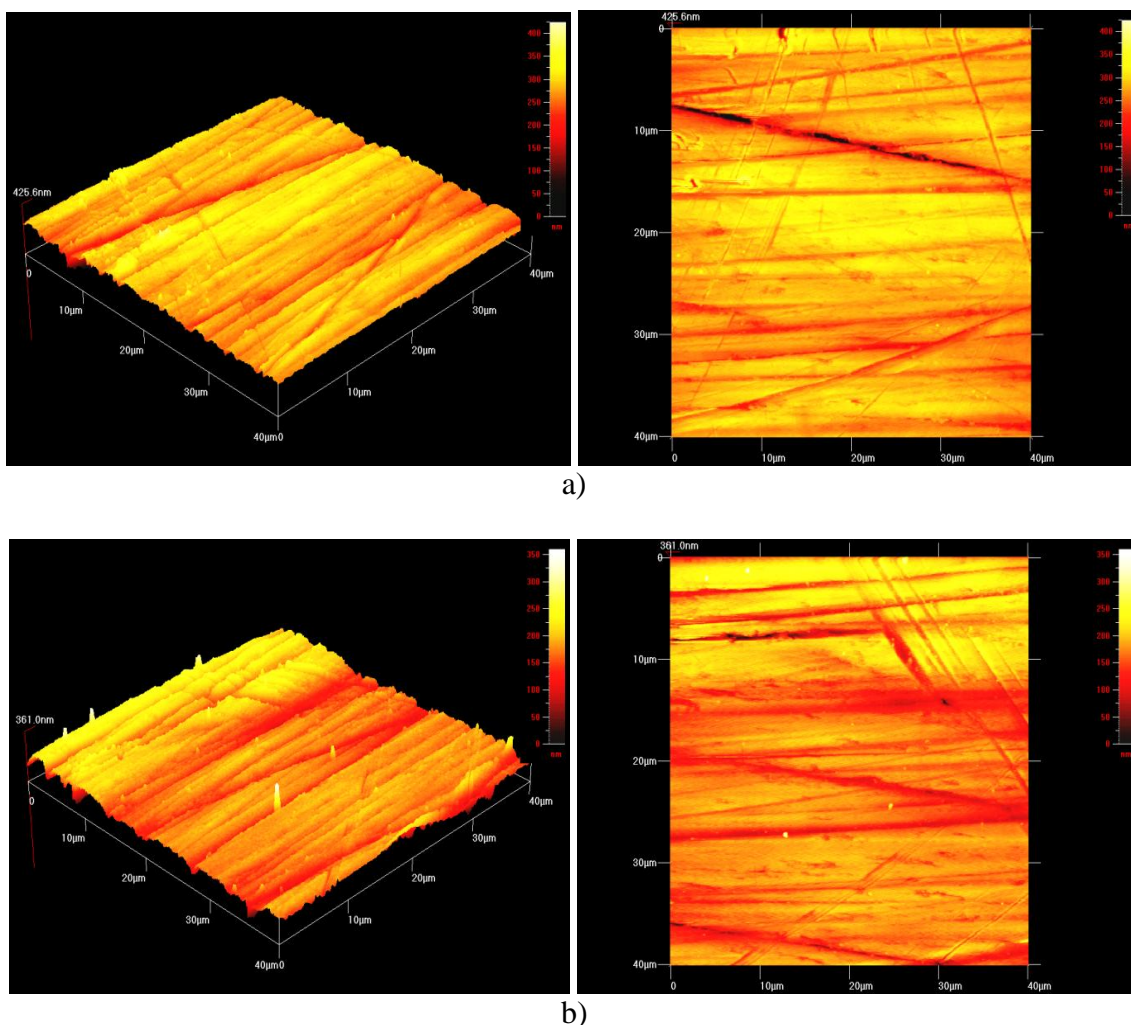


Figure 2. AFM image, a) main material surface b) welding seam surface.

3.2. SEM observations of the laser surface remelted and laser welded samples

The sample surfaces joined by CO₂ laser beam and the SEM images of the welding seams of samples whose surfaces had been modified via Nd:YAG laser at micro scale power intensities of 50W, 100W, and 150W are shown in Figure 3, and the results of elemental mapping analysis are shown in Figure 4. It is seen on the SEM images that the laser welding seam area on samples' surfaces expanded in line with an increase in the laser power, a homogeneous welding seam profile area formed, and no cracks or pores formed in the welding seams. The SEM images of the welding seam surface of the laser welded and surface modified sample numbered A3, whose surface was first sandpapered and polished with 3µ diamond paste and then electrolytically etched with oxalic acid can be seen in Figure 5 in detail.

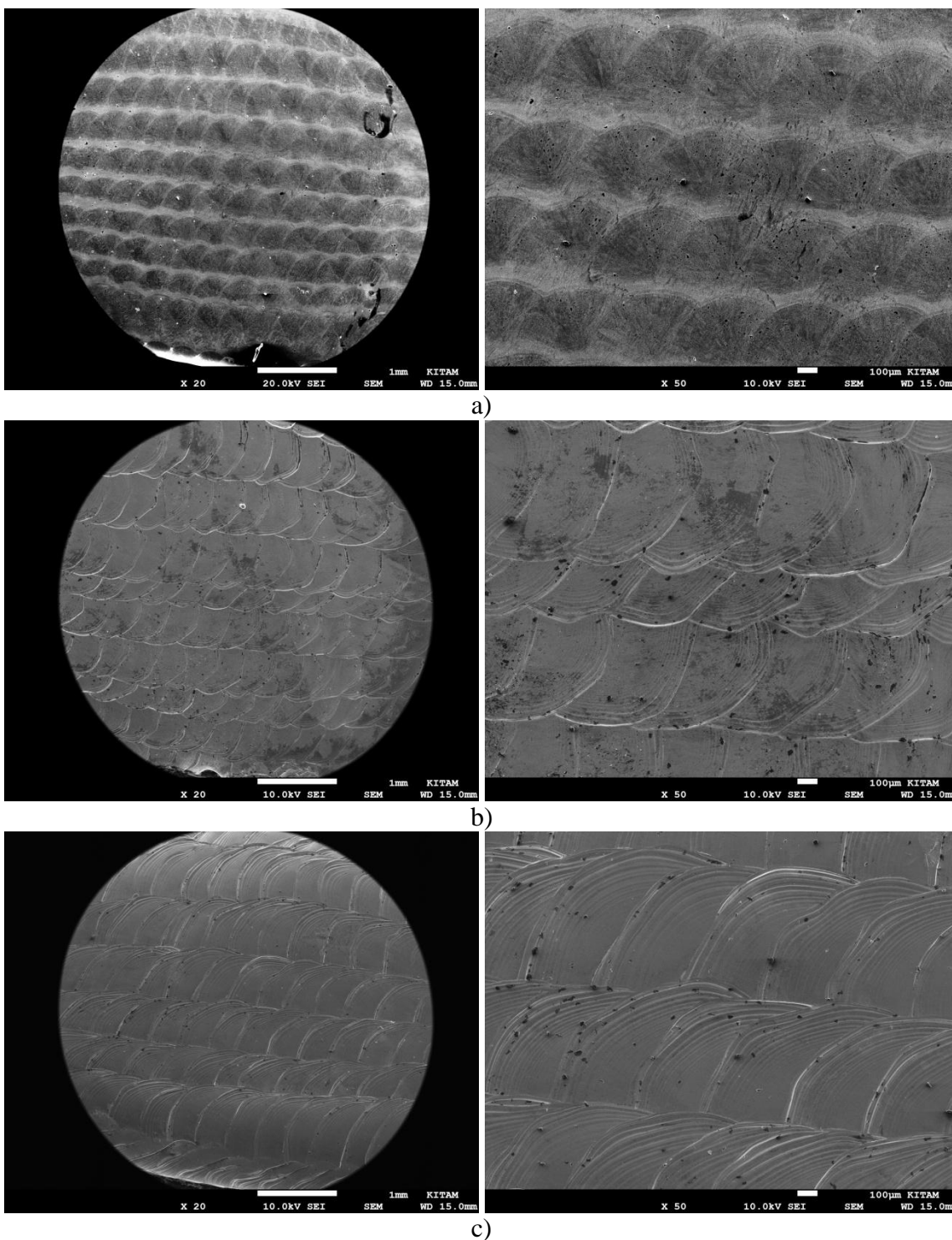
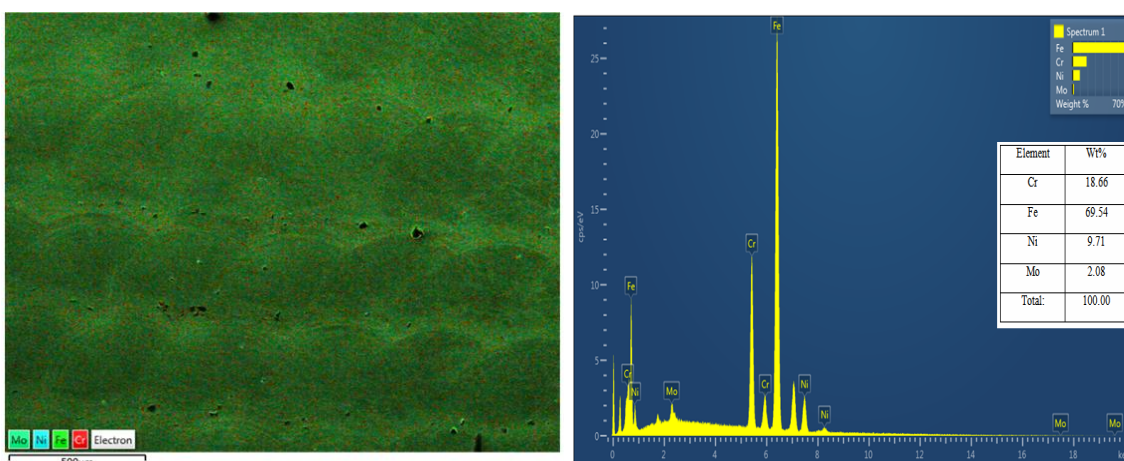


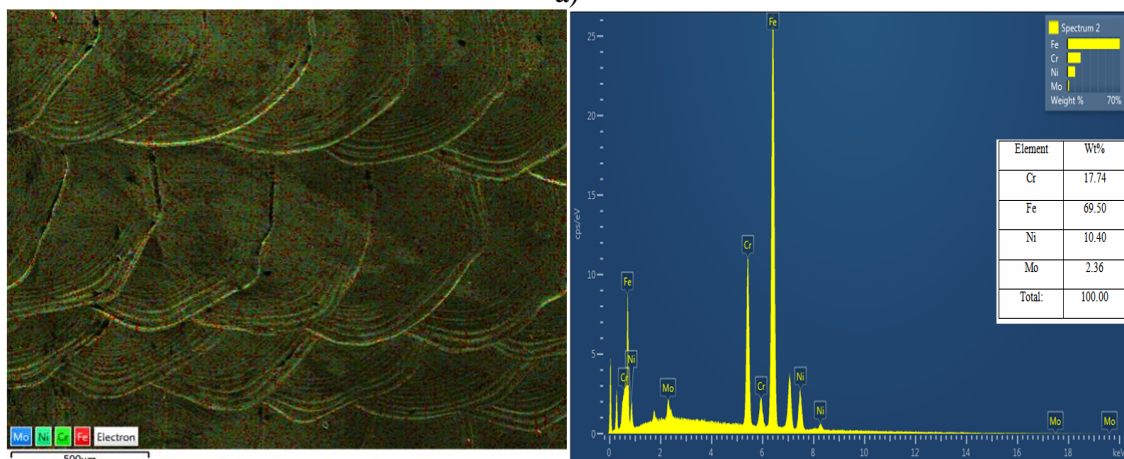
Figure 3. The SEM image of the welding seam surface of the laser surface remelted and laser welded samples, a) 50W, b) 100W, c) 150W laser surface modification parameters.

When the results of the elemental mapping (Figure 4) of the welding regions of the laser welded samples on the surfaces of which laser modification was applied were studied, it was seen that no loss of element due to surface modification via laser occurred in the areas that were analyzed, and that these results were in line with the results of the spectral analysis (Table 1) of the main material.

The application of surface modification procedures on laser welded sample surfaces via Nd:YAG laser with micro scale power intensity allowed minimal heat input to the sample surfaces, and prevented loss of element in the welding areas. It can be said that since no elemental loss occurred on the welding surfaces of the samples, they can output the resistance expected of them in corrosive environments. Previous studies have indicated that the improvement in corrosion resistance with laser surface treatment of austenitic stainless steel [18,30,31]. The corrosion resistance of stainless steels mainly depends on the composition of the passive oxide layer characteristics on their surface. An increase chromium content in the passive oxide layer, cause a better resistance to corrosion of stainless steels. Researchers has been reported to laser surface treatments caused an increasing in Cr content and oxide layer thickness of laser treated surfaces [18]. An increasing in Cr content and oxide layer thickness (mostly depends on the surface oxide film properties) ensures the corrosion resistance of stainless steel. In general, laser surface remelting (by using optimum laser process parameters) can lead to improvements in the corrosion behaviours, cavitation erosion resistance, tribological properties and biocompatibility (enhances adhesion, proliferation and spreading of cells on the laser treated surface of a biomaterial).



a)



b)

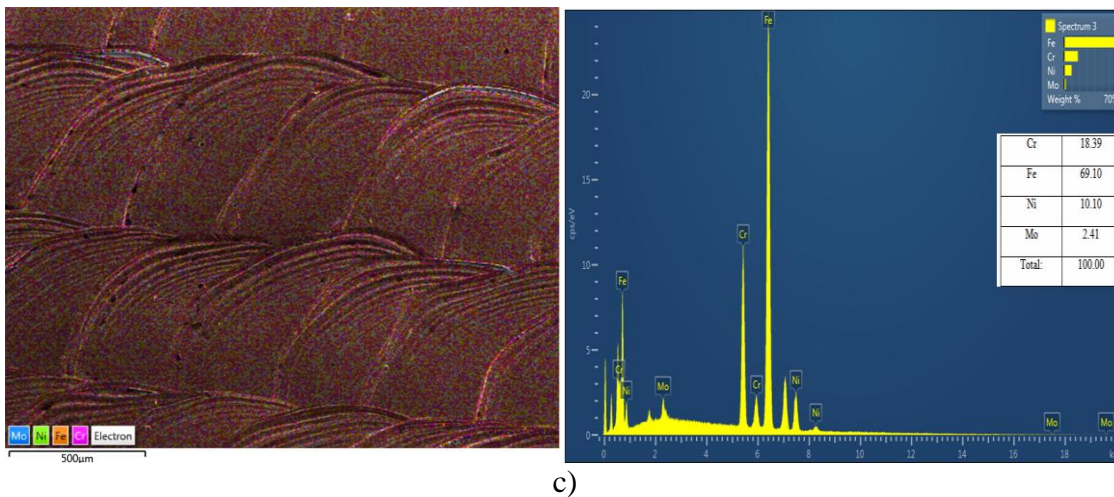


Figure 4. The results of the Elemental mapping of the welding seam surface of the laser surface remelted and laser welded samples, a) 50W, b) 100W, c) 150W laser surface modification parameters.

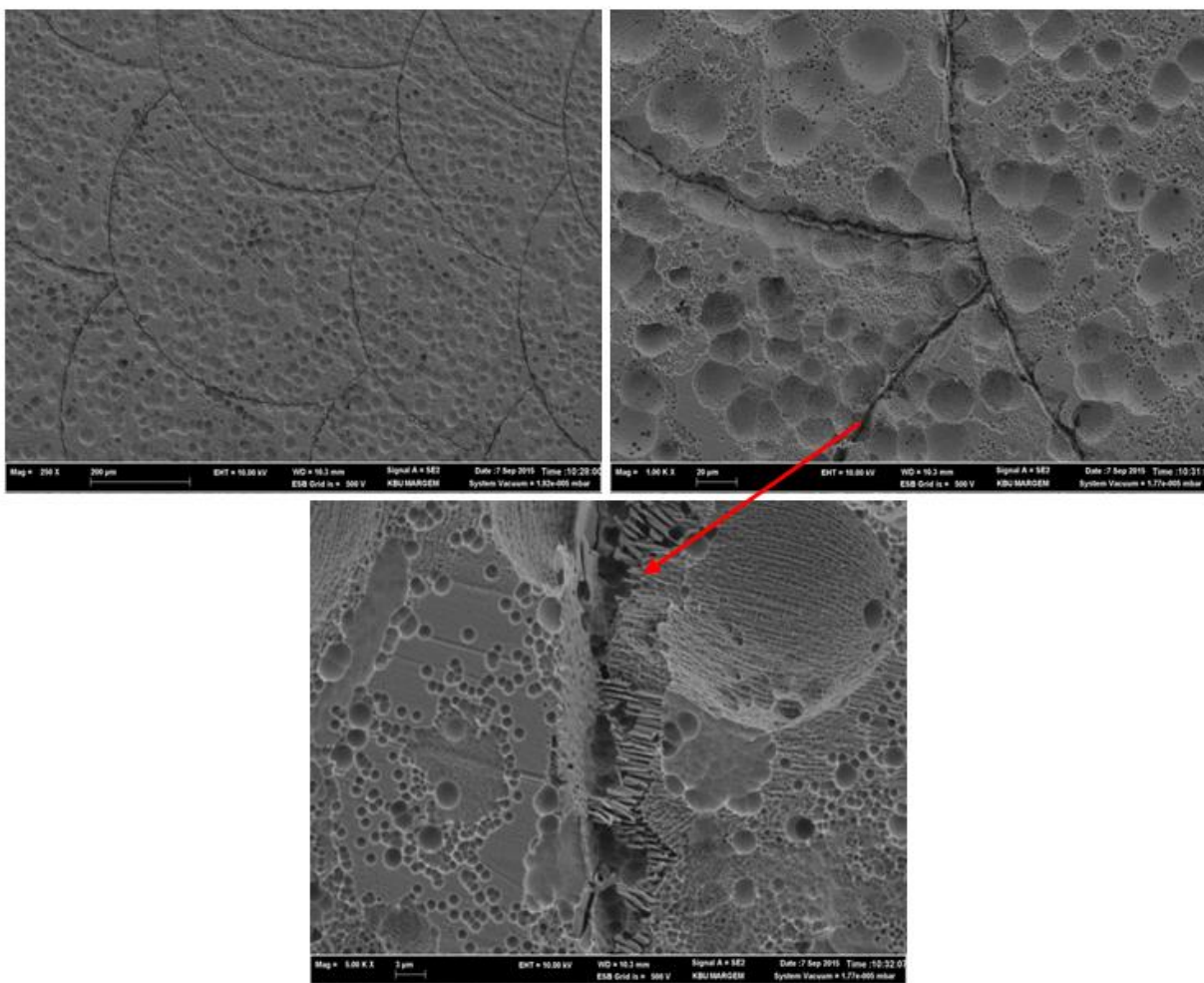


Figure 5. After the etching electrolytically SEM image of the welding seam surface of the laser surface remelted and laser welded A3 sample.

3.3. The AFM inspection of the laser surface remelted and laser welded samples

The average surface roughness values (R_a) of the laser welded samples, on whose surfaces laser modification had been applied, were identified via AFM analysis, and the obtained surface topography images are shown in Figure 6.

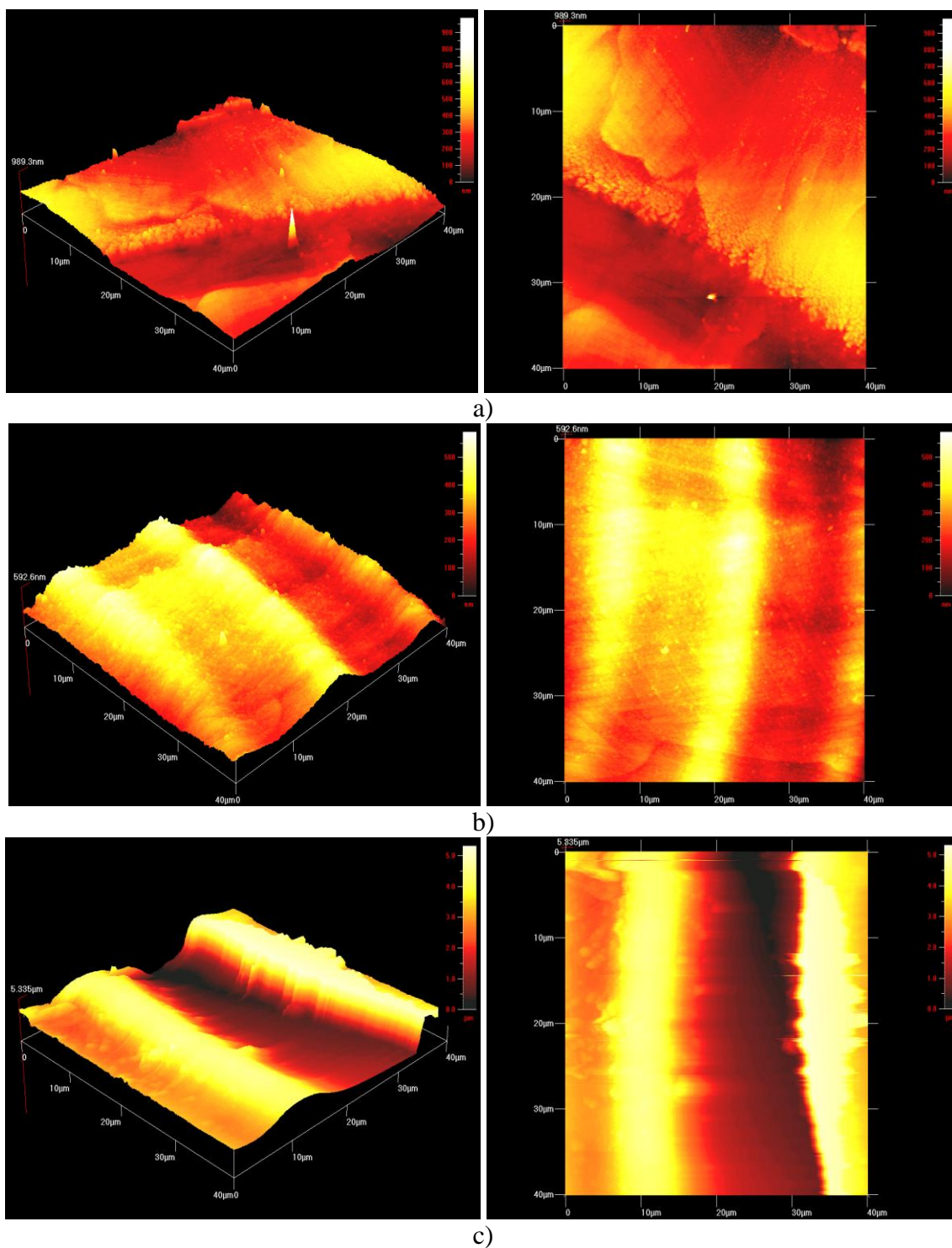


Figure 6. AFM image, welding seam surfaces of laser surface remelted and laser welded samples, a) 50W, b) 100W, c) 150W laser surface modification parameters.

The R_a value obtained on the welding seam surface of the sample on which surface modification via 50W laser power had been applied was found to be 59.4nm, the R_a value obtained on the welding seam surface of the sample on which surface modification via 100W laser power had been applied was found to be 87.4nm, and the R_a value obtained on the welding seam surface of the sample on which surface modification via 150W laser power had been applied was found to be 224nm. It is clearly seen in the results that the roughness of sample surfaces increase significantly depending on the power of laser welding.

3.4. XRD inspection

The formations that could occur in the weld metal and HAZ regions of the laser welded sample and on the surface of the laser surface remelted and laser welded sample, were inspected by means of the XRD method in the $30^\circ < 2\theta < 105^\circ$ interval, and the results are shown graphically in Figure 7.

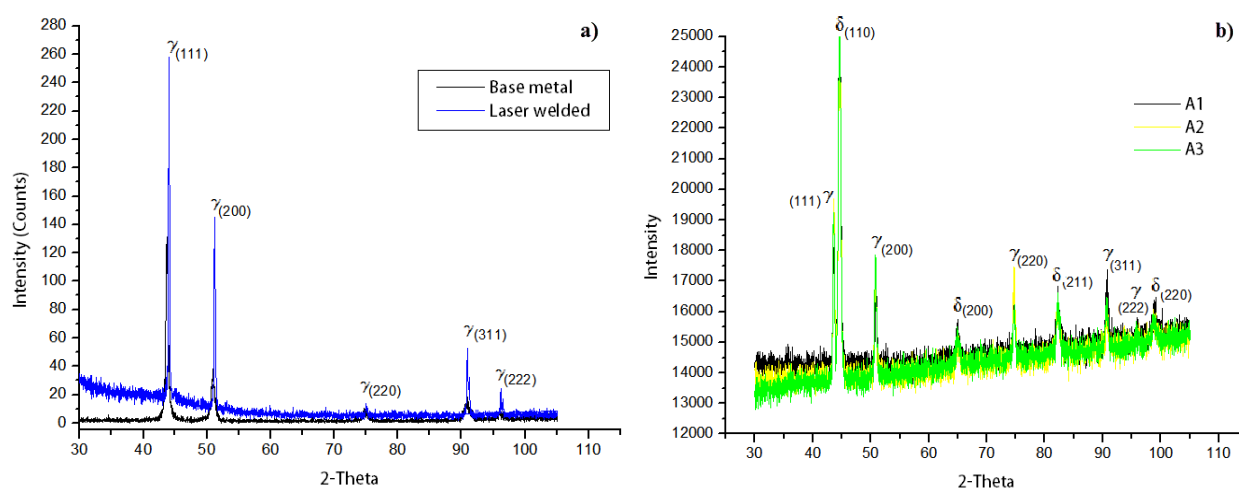


Figure 7. XRD result, a) laser welded sample, b) laser surface remelted and laser welded sample

When the peaks of the main material and the peaks of the welded sample are compared on the graph (Figure 7a), it is seen that the peaks of the welded sample are sharper and more frequent, as well as increases in the peak intensities. This situation may be linked to the changes that occurred in the crystal lattice parameters of the sample due to heat input. Undesired formations such as chromium-carbide precipitation ($M_{23}C_6$) in the weld metal and HAZ were not observed in the XRD patterns.

When the results of the XRD analysis (Figure 7b) of the laser welded samples on which laser surface modification was applied are compared with the peaks of the welded samples without laser surface modification, it is seen that the peaks of the welded samples with laser modification were sharper and more frequent, and also their peak intensities increased. Also, while peaks of austenite phase are dominantly seen in Figure 7a, the laser welded samples on which surface modification was applied show, in addition to peak formation due to austenite phase, peak formations of δ -ferrite as a proof of the crystallographic texture change of the surface (Figure 7b). It can be expected that δ -ferrite formation may lead to a little increase in hardness [22].

3.5. Observations of microhardness

When the average microhardness distribution of welded joint was inspected, it was observed that the main material hardness value was 200 HV, HAZ hardness value was 225 HV, and weld metal hardness value was 240 HV, respectively. It is understood that the hardness values of HAZ and the weld metal are close to each other, and that the hardness value of the main material is a little lower. It is assumed that the reason the hardness of the weld metal is higher than that of the main material is related to the microstructure of the weld metal with fine grain size obtained as a result of the rapid cooling and solidifying due to the low heat input. In the literature, it is shown that the main reason that leads to hardness in weld metal is the fine grain size structure [24,32]. It can be concluded that heat input has no significant effect on the fact that the HAZ values of welded joint and the hardness value of the weld metal are very close to each other because, since austenitic stainless steel does not go through any phase transformation, hard phases such as martensite are not expected to form in their structures; therefore, their hardness values happen to be close to each other. Even though small increases may be seen during the inspection of the hardness of the laser welded samples on which laser surface modification had been applied, these increases did not lead to significant changes in the hardness, and hardness values similar to the samples with no laser modification were found. Since austenitic stainless steel cannot be hardened via heat treatment and since sample surfaces are exposed to micro scale laser beam at low powers, no significant changes in their hardness values occurred.

4. CONCLUSIONS

In this study, we analyzed the surface changes that were obtained after surface remelting procedure was applied on the surfaces of laser welded samples via Nd:YAG laser, as well as the microhardness of surface characterization of AISI 316L stainless steel joined by CO₂ laser beam welding method, and the results are outlined below.

- It was observed that the HAZ hardness values of the laser welded sample and the weld metal were close to each other, and that the hardness value of the main material was a little lower. No significant difference was found between the microhardness values of the laser welded sample and the laser welded sample on which laser surface modification was applied.
- As a result of XRD inspection, while austenitic phase peaks were observed dominantly on the laser welded and non-laser welded samples on which no laser surface modification was applied, peak formations of δ -ferrite phase that prove the change in the crystallographic texture of the surface were observed in addition to the peak formations of austenitic phase. Also, undesired formations such as chromium-carbide precipitation ($M_{23}C_6$) in the laser welded samples with surface modification were not observed.
- It was observed that the average roughness value of the sanded laser welding seam surface was a little higher than the surface roughness value of the main material, and as a result of the heat input conducted to the welding area via the welding procedure, the welding seam affected the surface texture and it is considered to be the main reason why this result was obtained. It was

determined that the sample with the highest average surface roughness value was the laser welded sample on whose surface modification was applied via the highest laser power.

ACKNOWLEDGEMENTS

The author would like to express their thanks to Prof. Dr. Uğur Kölemen, and Dr. Fikret Yılmaz, Faculty of Arts and Sciences, Department of Physics, Gaziosmanpaşa University for the use of Atomic Force Microscope (AFM) equipment. The author would also like to thanks to KİTAM, Samsun Ondokuz Mayıs University for the use of SEM, XRD analysis.

References

1. M.B. Alexandru, C. Andrei, C. Marian, B. Zorica, R.C. Zizi, and S.E. Valentina, *Stainless Steel the Environment Friendly Choice*, Advances in Control, Chemical Engineering, Civil Engineering and Mechanical Engineering, Wseas Press, Spain (2010)
2. J.R. Davis, *Introduction to Stainless Steels*, Materials Park, Ohio, USA (2000)
3. J.R. Davis, *ASM Speciality Handbook: Stainless steels*, ASM International. Ohio, USA (1994)
4. R. Yılmaz, and M. Tümer, *Int. J. Adv. Manuf. Technol.*, 67 (2013) 1433
5. D. Özyürek, *Materials and Design*, 29 (2008) 597
6. H.J. Cross, J. Beach, L.S. Levy, S. Sadhra, T. Sorahan, and C. McRoy, *Manufacture, Processing and Use of Stainless Steel: A Review of the Health Effects*, Prepared for Eurofer by the Institute of Occupational Health, University of Birmingham (1999)
7. A. Balamurugan, S. Rajeswari, G. Balossier, A.H.S. Rebelo, and J.M.F. Ferreira, *Materials and Corrosion*, 59 (2008) 855
8. C.T. Kwok, *Laser Surface Modification of Alloys for Corrosion and Erosion Resistance*, Woodhead Publishing in Materials, Cambridge, UK (2012)
9. J.J. Kim, and Y.M. Young, *Int. J. Electrochem. Sci.*, 8 (2013) 11847
10. C.C. Shih, C.M. Shih, K.Y. Chou, S.J. Lin, and Y.Y. Su, *Journal of Biomedical Materials Research Part A*, 80 (2007) 861
11. D. Kuroda, S. Hiromoto, T. Hanawa, and Y. Katada, *Materials Transactions*, 43 (2002) 3100
12. Y.C. Tang, S. Katsuma, S. Fujimoto, and S. Hiromoto, *Acta Biomaterialia*, 2 (2006) 709
13. A. Kurella, and N.B. Dahotre, *Journal of Biomaterials Applications*, 20 (2005) 5
14. E. Chikarakara, N. Sumsun, and B. Dermot, *Applied Physics A: Materials Science & Processing*, 101 (2010) 367
15. L. Hao, J. Lawrence, Y.F. Phua, G.C. Lim, and H.Y. Zheng, *J Biomed Mater Res B Appl Biomater*, 73 (2005) 148
16. C.T. Kwok, F.T. Cheng, and H.C. Man, *Materials Science and Engineering A*, 290 (2000) 55
17. S.H. Alavi, and S.P. Harimkar, *Ultrasonics*, 59 (2015) 21
18. W. Pacquentin, N. Caron, and R. Oltra, *Applied Surface Science*, 288 (2014) 34
19. E. Chikarakara, N. Sumsun, and B. Dermot, *Applied Surface Science*, 302 (2014) 321
20. H. Zhang, J. Han, Y. Sun, Y. Huang, and Zhou M, *Materials Science and Engineering C*, 56 (2015) 29
21. R.K. Gupta, R. Sundar, B. Sunil Kumar, P. Ganesh, R. Kaul, K. Ranganathan, K.S. Bindra, V. Kain, S.M. Oak, and L.M. Kukreja, *JMEPEG*, 24 (2015) 2576
22. C.T. Kwok, K.H. Lo, W.K. Chan, F.T. Cheng, and H.C. Man, *Corrosion Science*, 53 (2011) 1591
23. C. Köse, and R. Kaçar, *Materials & Design*, 64 (2014) 226
24. C. Köse, and R. Kaçar, *Materials Testing*, 56 (2014) 785
25. C. Köse, and R. Kaçar, *Journal of the Faculty of Engineering and Architecture of Gazi University*, 30 (2015) 235
26. C. Köse, R. Kaçar, A.P. Zorba, M. Bağirova, and A.M. Allahverdiyev, *Materials Science and Engineering: C*, 60 (2016) 218

27. C. Köse, and R. Kaçar, *Int. J. Electrochem. Sci*, 11 (2016) in press.
28. M. Taskin, U. Caligulu, and M. Turkmen, *Materials Testing*, 53 (2011) 741
29. R.R.L. De Oliveira, D.A.C. Albuquerque, T.G.S. Cruz, F.M. Yamaji, and F.L. Leite, *INTECH Open Access Publisher* (2012)
30. I.Y. Khalfallah, M.N. Rahoma, J.H. Abboud, and K.Y. Benyounis, *Optics & Laser Technology*, 43(2011) 806
31. O. Vedat Akgün, M. Üregen, and A.F. Çakır, *Materials Science and Engineering: A*, 203 (1995) 324
32. P. Sathiya, and M.Y. Abdul Jaleel, *Optics and Lasers Technology*, 42 (2010) 968

© 2016 The Authors. Published by ESG (www.electrochemsci.org). This article is an open access article distributed under the terms and conditions of the Creative Commons Attribution license (<http://creativecommons.org/licenses/by/4.0/>).